Journal of Research and Applications in Mechanical Engineering
ISSN: 2229-2152 (Print); 2697-424x (Online)
(2024) Vol. 12, No. 2, Paper No. JRAME-24-12-030
[DOI: 10.14456/jrame.2024.30]

Research Article

Rolling Resistance Evaluation of Non-pneumatic Tire with Linked Zig-zag Structure using Scale Model

T. Suzuki[1,*], T. Okano[1], Y. Washimi[1], K. Sasaki[1], T. Tanimoto[1], K. Fujita[2], K. Yokoyama[3], K. Ushijima[4]

[1] *EV system Laboratory, Research Division, Nissan Motor Co., Ltd., Atsugi, 243-0123, Japan*
[2] *Department of Mechanical Engineering, National Institute of Technology, Ube College, Ube, 755-8555, Japan*
[3] *Department of Engineering, Graduate School of Tokyo University of Science, Tokyo, 125-8585, Japan*
[4] *Department of Engineering, Tokyo University of Science, Tokyo, 125-8585, Japan*

Received 18 January 2024
Revised 12 March 2024
Accepted 19 March 2024

Abstract:
In automobiles, it is increasingly important to reduce the frequency of maintenance due to accidental failures, and puncture-free non-pneumatic tires (NPT, airless tires) are expected to be used. We proposed a new NPT with a linked zig-zag structure to reduce rolling resistance (RR). Finite element analysis (FEA) results showed that NPT with a linked zig-zag structure can reduce RR more than other NPTs. The purpose of this paper is to verify the reduction of RR by the proposed structure using an actual machine. In order to verify the actual machine, we formulated the equivalent stiffness of the proposed structure and designed an actual scale model that can be prototyped. As a result of the rolling test, we were able to verify the reduction of RR in the scale model as well as the structural analysis.

Keywords: *Non-Pneumatic tire, Airless tire, Rolling resistance, Energy loss, Equivalent stiffness*

1. Introduction

In the field of automobiles, it is increasingly important to reduce the frequency of maintenance due to accidental failures and achieve puncture-free tires. With this background, non-pneumatic tire (NPT, also known as an airless tire) is expected to be increasingly utilized. Pneumatic tires have four major functions, which are to hold the vehicle weight, transfer the driving/braking force to the ground, transfer the road reaction force of steering to the vehicle, and to absorb vibration caused by roughness of the road surface. Conventional pneumatic tires use the pressure of air filled in a tire to perform four major functions, while NPTs use only deformation of component parts. The basic structure of NPT is shown in Fig. 1 [1, 2]. NPT is made of three main parts: a wheel, body parts, and a tread ring. The elastic deformation of a tread ring and body parts enables the tire to perform four major functions. In Fig. 1(b), F_z means the wheel load, and f_r means the radial force received by the radially extending spokes. The load F_z is supported mainly by the tension of the upper half of the top body parts. Such a load carrying mechanism is called "Top Loaders" [2]. This concept supports the wheel load by tension in the ungrounded region of the spokes extending radially from the wheel mounted on the vehicle body. This concept requires a very rigid treadling, which makes it difficult to achieve ride comfort performance. On the other hand, an airless tire with a honeycomb structure applied to the body part has been proposed [3, 4]. The honeycomb structure easily deforms only the body part near the ground, so it is difficult to support loads in the ungrounded body part. Furthermore, a structure in which the unit cell is modified from a hexagonal column has also been proposed [5, 6]. The new unit cell structure has the potential to

* Corresponding author: T. Suzuki
E-mail address: takuma_s@mail.nissan.co.jp

outperform pneumatic tires, but it faces manufacturing challenges due to its complex structure. Other types are referred to as convex-type and solid-type [7].

Since NPT has a structure that supports loads only by deformation of the tire, energy loss due to deformation of members tends to be large. In the study of rolling resistance of airless tires, the spoke structure [8], honeycomb structure [9, 10] and hexagonal lattice spoke [11] have been investigated using a method that calculates the total energy loss during static tire deformation by structural analysis. All of them demonstrate the reduction of rolling resistance by altering the dimensions and specifications of each structure. However, there is no example that examines the difference in rolling resistance due to differences in topology, and the concept to reduce rolling resistance is unclear. While many studies have measured the rolling resistance of pneumatic tires [12-15], there are few studies that have verified the rolling resistance in NPT through experimentation.

To reduce rolling resistance in NPT, this study proposes an NPT with a zigzag connected structure. The purpose of this paper is to verify the reduction of rolling resistance (RR) by the proposed structure using an actual machine. To evaluate the effectiveness of the proposed NPT in reducing RR, two scale models of the proposed NPT and the conventional NPT were designed respectively. The equation of equivalent stiffness is utilized in the design of the proposed structure. The two scale models are designed to be approximately equal in vertical stiffness of the tire. First, two scale models are evaluated by structural analysis on static load. Next, the scale models are prototyped by vacuum injection. Finally, the reduction in rolling resistance is verified by a rolling test using the prototype.

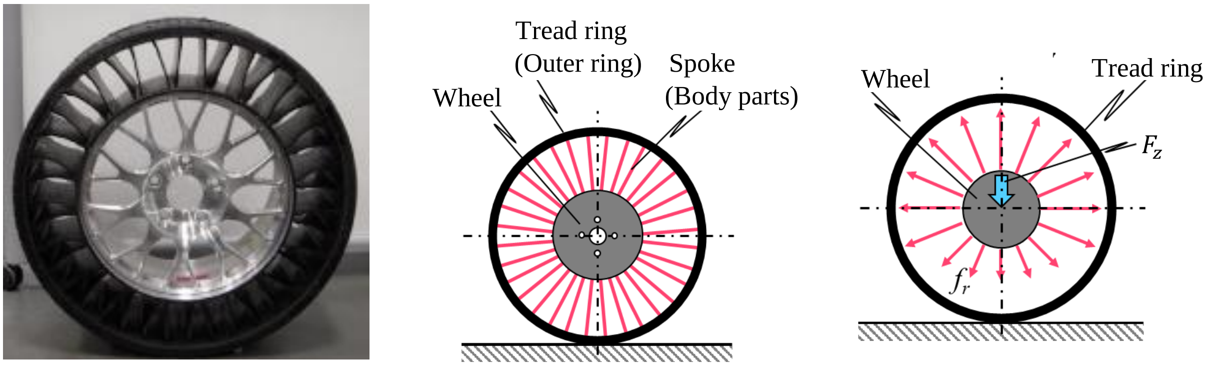

(a) Spoke type [1]   (b) Schematic diagram   (c) Top loaders [2]

Fig. 1. Non-pneumatic tire for passenger vehicle

2. Conventional Non-Pneumatic Tires and a New Concept

2.1 Issue of Conventional Non-Pneumatic Tires

To address the issue of NPTs, conventional NPTs were applied to a small passenger car. Various types of NPTs have been proposed, with the spoke type being considered conventional in this study. Fig. 2(a) depicts the simplest type, known as the vertical spoke type. This configuration is prone to buckling deformation of the spokes near the ground. To mitigate buckling deformation, spokes must possess a structure that dictates the direction of deformation. The structure shown in Fig. 2(b), which experiences fewer instances of buckling, is designated as the conventional NPT. Fig. 2(b) is referred to as the sloping spoke type. To elucidate the issue with conventional NPTs, this type of tire was designed, with requirements set for load holding and shock absorption. ABAQUS/Standard was employed for finite element analysis (FEA).

(a) Vertical spork type (b) Sloping spoke type

Fig. 2. Conventional non-pneumatic tires with different body parts

Fig. 3 illustrates vertical load ratios on the outer surfaces of the wheels. Due to the elevated vertical load values near the ground, this scenario corresponds to a bottom loader configuration, as depicted in Fig. 4. In Fig. 4, F_z denotes the tire's vertical force supported by each spoke. If the stiffness of the tread ring is increased, this configuration would resemble a top loader concept. However, increasing the stiffness of the tread ring to meet envelope characteristics for ride comfort is not feasible. Conventional NPTs face the challenge of having a high vertical load ratio near the ground. Therefore, it is crucial to distribute the wheel load across the entire body of the tire for enhanced durability and reduced rolling resistance.

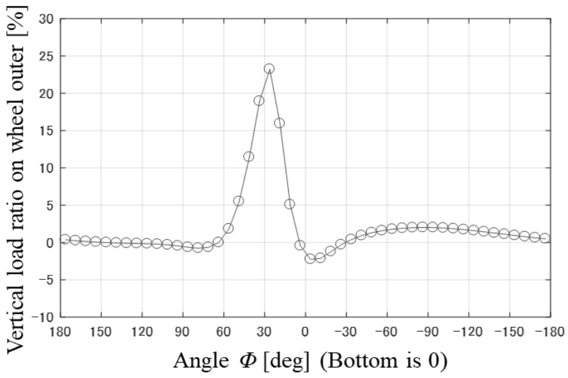

Fig. 3. Vertical load ratios of sloping spoke type

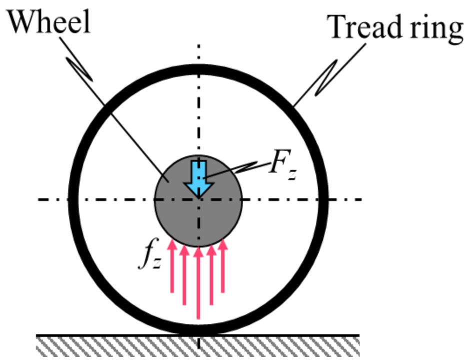

Fig. 4. Bottom loader

2.2 Non-Pneumatic Tire with Linked Zig-Zag Structure

To achieve a structure capable of distributing the wheel load both at the bottom and the top, we explored a concept that efficiently utilizes circumferential load transfer, as illustrated in Fig. 5. In Fig. 5(b), "f_c" represents the circumferential internal force on the body. When only radial members are present, wheel loads tend to concentrate near the ground. The inclusion of circumferential members connecting the spokes can mitigate this issue. Building upon this concept, we introduced a new structure depicted in Fig. 6 [16]. The proposed structure features zigzag spokes and intermediate rings that connect to adjacent zigzag spokes. The wheel load resulting from spoke deformation is transferred to the top of the tire through these intermediate rings. In section 2.1 of the study, the vertical load ratio was analyzed using finite element analysis (FEA). This analysis demonstrated that the proposed structure has the capability to distribute the wheel load across the top of the body, as demonstrated in Fig. 7.

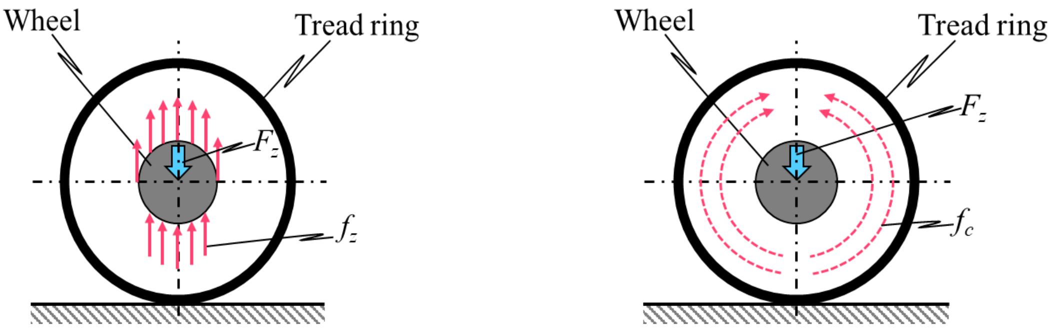

(a) Top and Bottom loader (b) Circumferential load transfer

Fig. 5. New concept of NPT

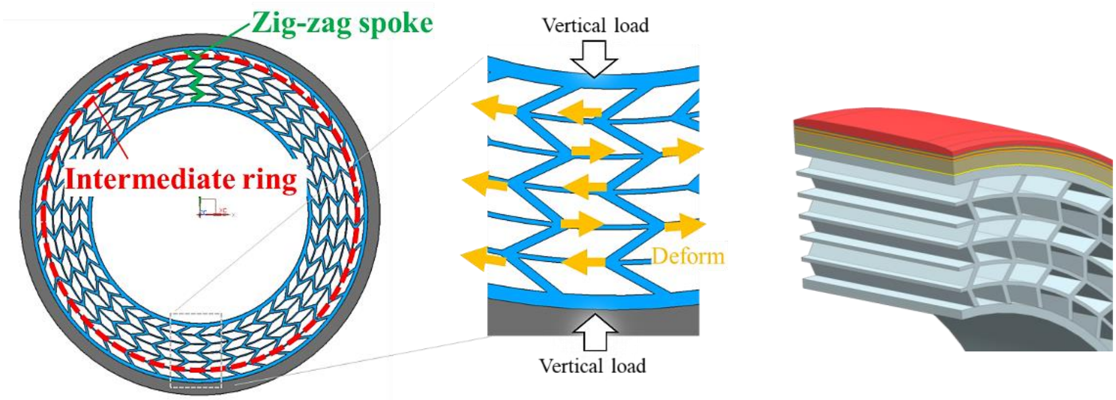

Fig. 6. Proposed structure (Linked zig-zag structure) [16]

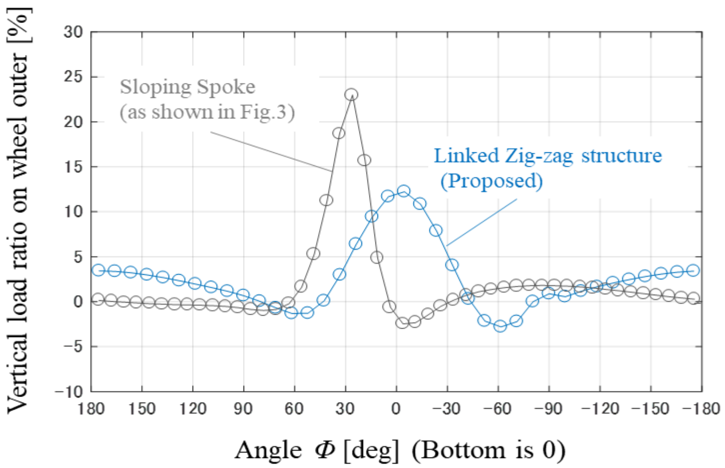

Fig. 7. Comparison of vertical load ratios (Proposed structure vs. Conventional)

3. Principal Evaluation Model Design

To assess the efficacy of the proposed structure in reducing rolling resistance, we developed a scaled prototype evaluation model of the proposed NPT, enabling rolling tests on real machines. Additionally, we designed a conventional sloping spokes type as a reference NPT for comparison purposes.

3.1 Dimension and Material Properties

The dimensions of the principal evaluation model are outlined in Table 1. The model's overall size was set to be 33% of a standard passenger car tire, with the tread ring thickness defined as 5 mm. Typically, the tread rings of conventional NPTs are composed of a composite material comprising rubbers and reinforcing materials. For this study, a specific type of resin was chosen for the tread ring to facilitate prototype production. The material selection was based on equivalent stiffness values derived from the thickness and stiffness properties of rubber and reinforcing materials. Material properties are detailed in Table 2.

Table 1: Dimensions of principal evaluation model

Diameter [mm]	200
Width [mm]	49.3
Thickness of tread ring [mm]	5

Table 2: Material properties

	Young's modulus [MPa]	**Poisson's ration [-]**	**tanδ [-]**
Body parts	40	0.33	0.177
Tread ring	500	0.33	0.366

3.2 Design of the Proposed NPT

Designing a new NPT using FEA can be a time-consuming endeavor, requiring careful consideration of both topology and the dimensions of the tire's body parts. However, if the structure of the body parts can be formulated in a mechanical model, the design process can be significantly expedited [3, 17, 18]. Our proposed structure is notably intricate, involving a multitude of parameters such as thickness and angle that need adjustment to attain the desired vertical spring characteristics. Consequently, the utilization of CAD for geometry modeling and structural analysis for iterative refinement becomes imperative. To enhance the efficiency of the design process and reduce the number of study cycles, we concentrated on conceptual design using the equivalent stiffness E^* of the unit cell. This method is applied solely during the initial design phase, with comprehensive analyses performed subsequently through structural analysis.

The unit cell of the proposed structure comprises a rhombic shape, and an equivalent stiffness equation is derived based on the mechanics of elasticity of a tilted beam. Illustrated in Fig. 8(a), the proposed structure features inclined beams of length H (AB and BC in the figure) at an angle θ to the y-axis, along with horizontal beams BD of length L in the x-direction. The equivalent stiffness of the radial direction can be determined from the bending deformation of the inclined beams, as depicted in Fig. 8(b) and described by equation 1 [19]. This equation allows for the straightforward design of topology and dimensions to achieve the desired equivalent stiffness.

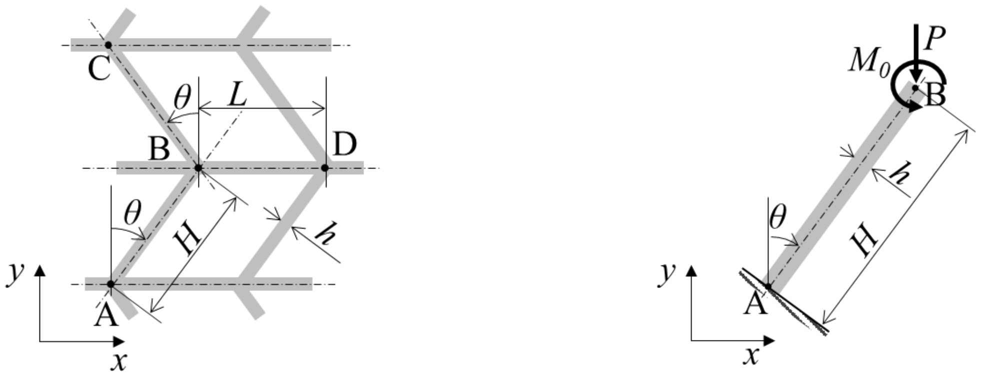

(a) Zig-zag structure (b) Incline beam

Fig. 8. Theoretical model for a linked zig-zag structure [20]

$$E^* = \frac{E_s(N+1)h^3\cos\theta}{(NL+H\sin\theta)H^2\sin^2\theta} \quad (1)$$

The basic design of the structure was conducted using equation (1), where E_s is the Young's modulus of the material, h is the thickness of the zig-zag spoke, and N is the number of unit cells on the x-axis. The detailed dimensions were determined by structural analysis to achieve a tire deflection of 4 mm (100 N/mm longitudinal spring) for a wheel load of F_z 400 N. The dimensions of the unit cell are values that can be manufactured via vacuum casting using silicon molds. The designed shape is depicted in Fig. 9(b).

3.3 Design of a Conventional NPT

To compare with the proposed structure, the conventional NPT with the sloping spokes shown in Fig. 2(b) was designed. The outer dimensions, material properties, and target longitudinal spring characteristics were equivalent to those of the proposed structure and spoke thicknesses that could be prototyped by vacuum casting was selected. The designed shape is shown in Fig. 9(a).

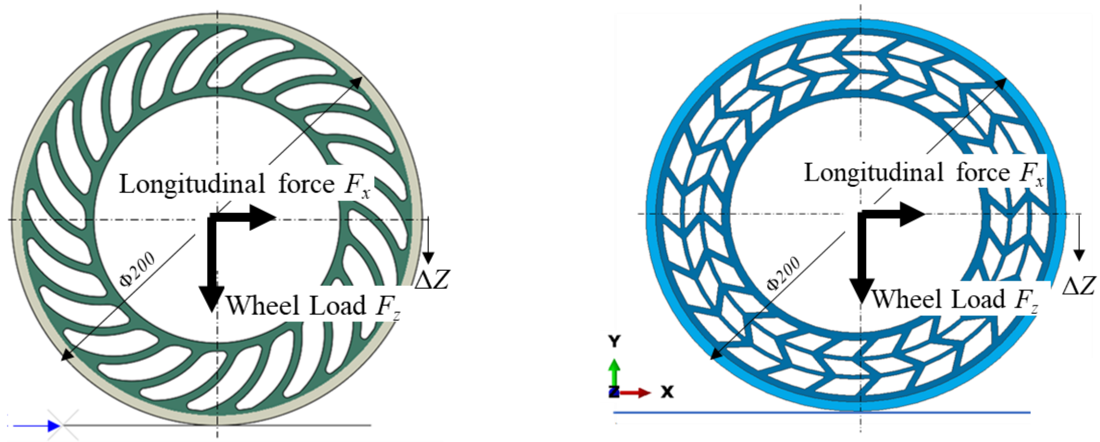

(a) Conventional structure

(b) Proposed structure

Fig. 9. Designed Non-pneumatic tire (Scale model)

4. Comparison with Structural Analysis

The two structures designed in Section 3 are compared by static analysis using ABAQUS/Standard.

4.1 Tire Vertical Stiffness

The vertical stiffness of both structures for the target is shown in Fig. 10. In real NPTs for passenger cars, the nonlinear curves of tire deflection by the wheel load vary depending on the structure of the body parts. This was also verified in the scale model.

4.2 Longitudinal Force by Wheel Load

In the case of a typical pneumatic tire, the force acting in the longitudinal direction of the tire is nearly zero even with an increase in wheel load. However, this differs for NPTs. In the case of NPTs, as depicted in Fig. 11, it was observed to be non-zero. With the sloping spoke structure, deformation of the spokes generates a longitudinal force in the tire, resulting in a longitudinal force equivalent to up to 10% of the wheel load.

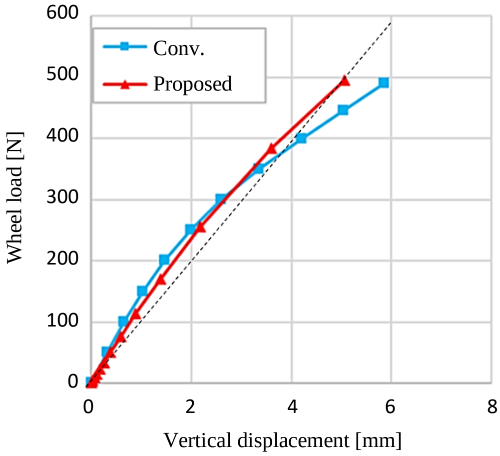

Fig. 10. Tire Stiffness (FEA)

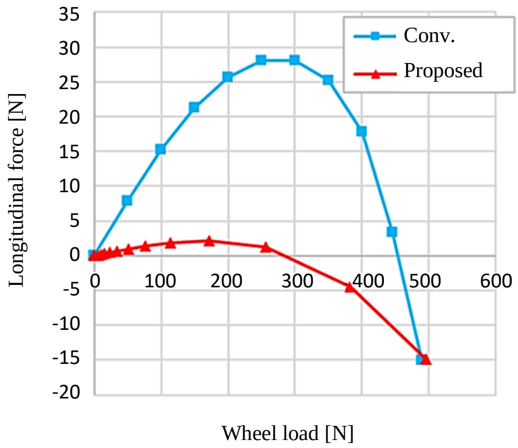

Fig. 11. Longitudinal force by wheel load (FEA)

4.3 Von Mises Stresses

Mises stresses on the deformation shape when the load is set to 400 N are depicted in Fig. 12. It was observed that stresses tended to concentrate more around the contact area in a limited number of spokes in the conventional structure compared to the proposed structure. Moreover, in the proposed structure, stress also acts on the intermediate ring along a circumferential direction, facilitating the transfer of the wheel load toward the top of the tire through the intermediate ring, as illustrated in the concept diagram in Fig. 4.

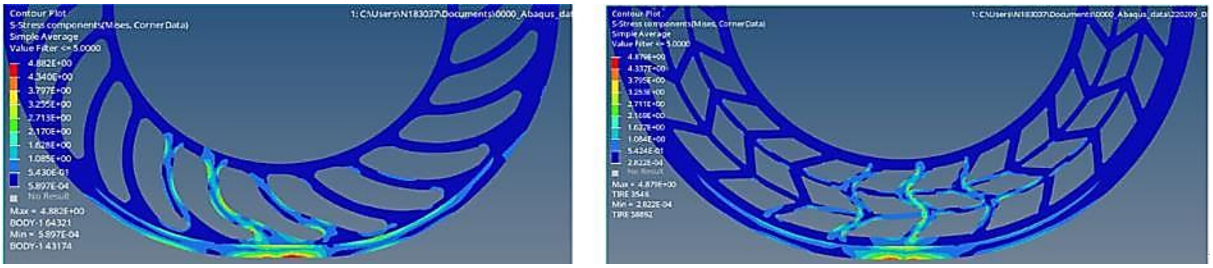

(a) Conventional structure (b) Proposed structure

Fig. 12. Misess Stress (FEA)

4.4 Rolling Resistance

The rolling resistance of a tire can be composed of three components as follows: energy loss due to parts deformation, road friction, and aerodynamic drag [12, 15]. There are two main methods for calculating rolling resistance (RR) using Finite Element Analysis (FEA). The first method simulates the rolling condition of a tire and directly computes the tire force in the contact area between the tire and the road. The second method calculates RR indirectly from the energy loss inside the tire, which is the primary factor contributing to RR. In this study, RR was defined by the energy loss obtained using static FEA based on the second method. The loss energy of the tire, St, can be calculated by integrating the strain energy, Se, and the material loss tangent, tanδwith the total tire volume *v*:

$$S_t = \int_v S_e \, tan\delta \, v \tag{2}$$

The Rolling Resistance Coefficient (*RRC*) is calculated by dividing the *RR* by the wheel load F_z. *RR* is calculated by dividing the energy loss S_t by the tire circumference length L_t [10, 15]:

$$RRC = \frac{RR}{F_z} \stackrel{\text{def}}{=} \frac{S_t/L_t}{F_z} \tag{3}$$

At each wheel load, the strain energy S_e is calculated using ABAQUS. The loss energy S_t is derived from the sum of the total strain energy S_e for each material, and tanδin Table 2. The RRC calculated using the values for the body, tread ring, and overall tire is shown in Fig. 13. At a wheel load of 500 N, the RRC of the proposed structure is 25% smaller than that of the conventional structure. Even though the tread ring has the same structure, the proposed structure has a smaller RRC than the conventional structure calculated by the strain energy of the tread ring.

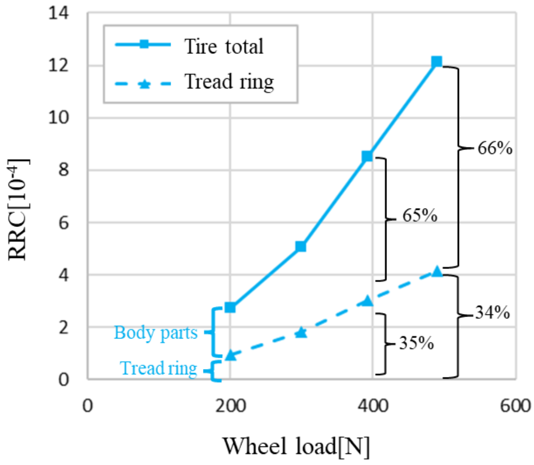

(a) Conventional structure

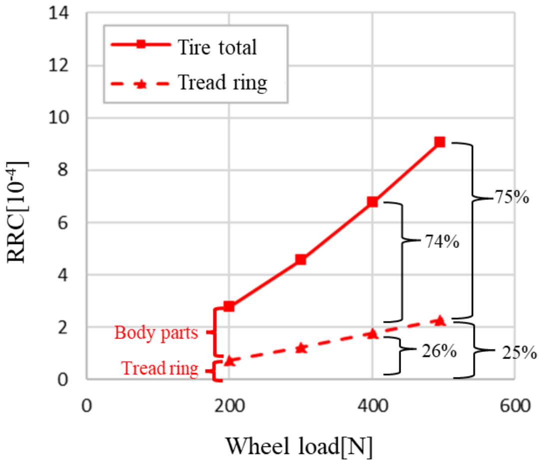

(b) Proposed structure

Fig. 13. Rolling Resistance Coefficient (FEA)

5. Validation of Design Concept in Rolling Tests

Principal evaluation models are self-manufactured and measured in rolling tests to validate the design concept experimentally.

5.1 Principal Evaluation Model

Specifications of principal evaluation models are shown in Table 3. The exterior appearance of the models is depicted in Fig. 14. The body parts and tread rings are made of urethane resin with the characteristics listed in Table 2. The models are manufactured using vacuum injection, ensuring mechanical connection between the wheels and body parts, while the body and tread rings are bonded through two-color molding.

Table 3: Specification of scale model

Material4	Wheel	Aluminum alloy (A6063)
	Spoke	Urethane resin, UPX8400(Sika Japan Ltd.), Compounding ratio A:B:C=100:100:35 Shore A hardness: 83
	Tread ring	Urethane resin, UP5690(Sika Japan Ltd.), Compounding ratio A:B:C=100:100:97 Shore D hardness: 90
Manufacturing		Sanjyu co. Ltd, Plamerry design co. Ltd.

(a) Conventional structure (b) Proposed structure

Fig. 14. Principal evaluation model for rolling test

5.2 Test Bench

The rolling test was conducted on a test bench as depicted in Fig. 15. The models were secured to an axle of the jig, pressed against the drum, and rotated by it. The models rotated passively as the drum was rotated by the drive motor. Vertical wheel load and rolling resistance force were measured by a load cell, as outlined in Table 4. The wheel load and rolling resistance were measured using a load cell equipped with the axle. The wheel load was adjusted by changing the length of the adjustable bolt to achieve the specified wheel load. The rotation speed was set using the motor's control system.

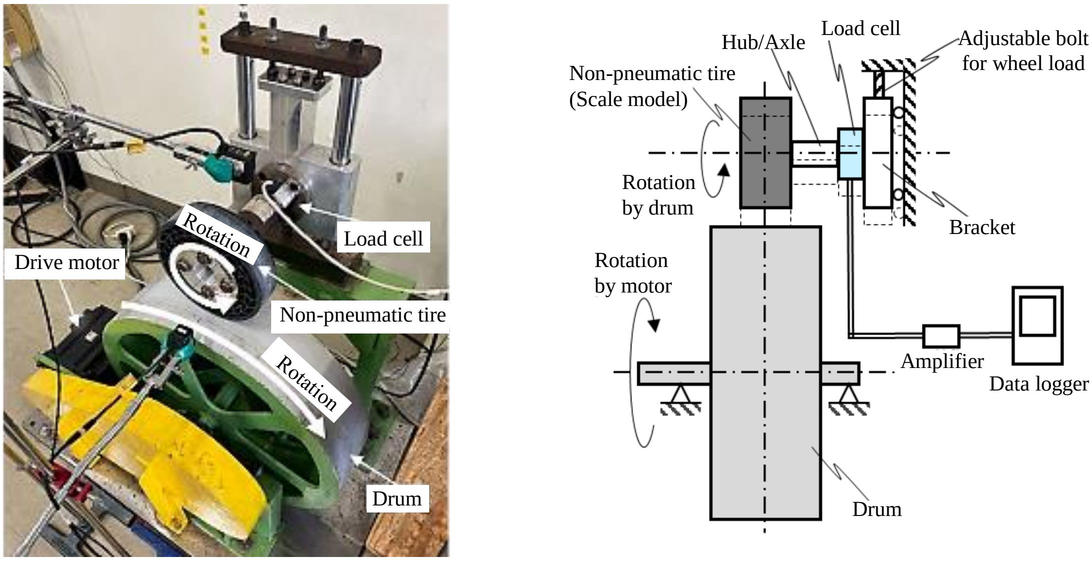

(a) Overall view (b) Schematic diagram

Fig. 15. Experimental equipment

Table 4: Specification of Load cell

Manufacturer	Kyowa Electronic Instruments Co., Ltd.	
Model	LFM-A-3KN	
Type	6-component force transducers	
Specification	Capacity	±3,000N, ±100Nm
	Non-linearity	<±0.5%
	Hysteresis	<±0.5%
	Coherence	<±1.5%
	Natural Frequency	5kHz

5.3 Measurements Results

For each scale model, rolling tests were conducted under two conditions of wheel load and three conditions of rotation speed. To ensure stable data under each condition, load measurements were taken after 10 minutes of rotation. The results of RRC measurements are presented in Fig. 16. In both scale models, RRC increased with increasing wheel load and rotation speed. The increase in RRC with wheel load was attributed to a shift in the stiffness of the material near the nonlinear region. The increase in RRC with rotational speed was due to increased heat generation caused by high deformation cycles. Under conditions where the wheel load exceeded 500 N, the RRC of the proposed NPT model was approximately 12% smaller than that of the conventional NPT. These results from rolling tests and FEA confirmed that the proposed model has a lower RRC compared to the conventional NPT. However, there was a significant difference between the absolute values of RRC obtained in rolling tests and FEA. Correlation of FEA will be conducted as future work for further RRC improvement.

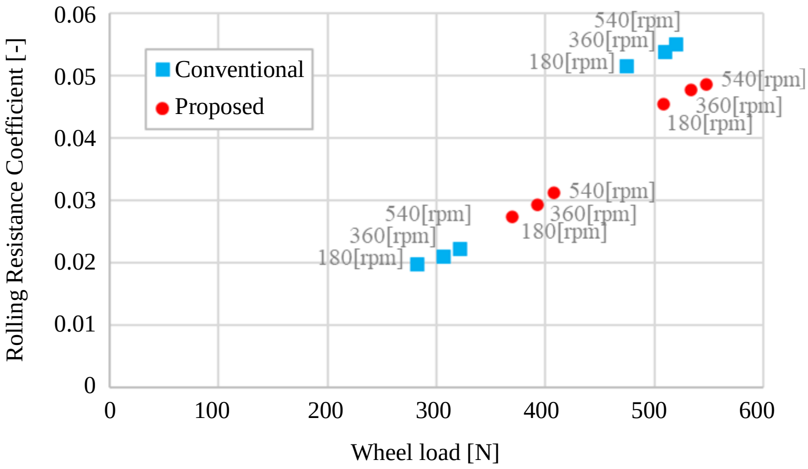

Fig. 16. Rolling Resistance Coefficient (Experiment, 6 conditions for each scale model)

6. Conclusion

In this paper, a novel low Rolling Resistance Coefficient (RRC) NPT utilizing the linked zig-zag structure is proposed. This structure can transfer the applied load weight from the bottom to the top, thereby relieving local stress concentration and reducing RRC. The effect of the structure on RRC reduction is studied using Finite Element Analysis (FEA), and it is also experimentally evaluated using the principal evaluation model scaled to 33% of the NPT targeting passenger cars. The results obtained from the FEA calculation and the experiment are as follows.

- The Rolling Resistance Coefficient (RRC) of the NPT with the proposed structure is calculated based on the strain energy obtained from static Finite Element Analysis (FEA). The result shows a 25% reduction in RRC compared to that of the conventional NPT designed to satisfy almost the same vertical stiffness as the proposed tire.
- The Rolling Resistance Coefficient (RRC) of the principal evaluation model is applied to the rolling tests to obtain its RRC experimentally. The result shows a 12% smaller RRC compared to that of the conventional NPT, consistent with the results obtained from the static FEA.

A detailed study will be conducted to clarify the reasons for the difference between the calculated and experimental results, aiming for further improvement in RRC as future work.

Nomenclature

E_s	Young modulus, MPa
E^*	Equivalent stiffness of Zig-zag structure, MPa
f_c	Circumferential internal force on body, N
f_r	Radial *i*nternal force on wheel outer, N
f_z	Vertical internal force on wheel outer, N

F_x Longitudinal force at wheel center by wheel load, N
F_z Wheel load, N
h Thickness of spoke, mm
H Inclined Spoke length, mm
L Intermediate ring length, mm
L_t Tire circumference length, mm
M_0 Input moment on inclined beam, Nm
N *N*umber of unit cell of Zig-zag structure on x- axis (Fig. 8)
P Input load on inclined beam, N
RR Rolling resistance, N
RRC Rolling resistance coefficient (RR/F_z)
S_e *S*train energy of each part, Nm
S_t Loss energy of tire, Nm
v Tire volume of each part, mm^3
ΔZ Vertical deformation of wheel center by wheel load, mm
$\tan\delta$ Material loss tangent
θ Spoke angle, deg
Φ Wheel angle, deg

References

[1] Narasimhan A, Ziegget J, Thompson L. Effects of material properties on static load-deflection and vibration of a non-pneumatic tire during high-speed rolling. SAE Int J Passeng Cars – Mech Syst. 2011;4(1):59-72.
[2] Rhyne TB, Cron SM. Development of a non-pneumatic wheel. Tire Sci Technol. 2006;34(3):150-169.
[3] Pewekar MM, Gaikwad SD. Strength validation of hexagonal cellular spoked non-pneumatic tires for automobiles through finite element analysis. Int J Sci Res Sci Technol. 2018;4(5):1044-1055.
[4] Deng YJ, Zhao ZQ, Lin F, Zang LG. Influence of structure and material on the vibration modal characteristics of novel combined flexible road wheel. Def Technol. 2022;18(7):1179-1189.
[5] Ju J, Kim DM, Kim K. Flexible cellular solid spokes of a non-pneumatic tire. Compos Struct. 2012;94(8):2285-2295.
[6] Zhang Z, Fu H, Liang X, Chen X, Tan D. Comparative analysis of static and dynamic performance of non-pneumatic tire with flexible spoke structure. J Mech Eng. 2020;66:458-466.
[7] Deng Y, Wang Z, Shen H, Gong J, Xiao Z. Comprehensive review on non-pneumatic tyre research. Mater Des. 2023;227:11742.
[8] Veeramurthy M, Ju J, Tompson LL, Summers JD. Optimization of geometry and material properties of a non-pneumatic tyre for reducing rolling resistance. Int J Veh Des. 2014;66(2):193-216.
[9] Aboul-Yazid AM, Emam MAA, Shaaban S, El-Nashar MA. Effect of spokes structures on characteristics performance of non-pneumatic tires. Int J Automot Mech Eng. 2015;11:2212–2223.
[10] Jin X, Hou C, Fan X, Sun Y, Lv J, Lu C. Investigation on the static and dynamic behaviors of non-pneumatic tires with honeycomb spokes. Compos Struct. 2018;187:27-35.
[11] Kim K, Heo H, Uddin MS, Ju J, Kim DM. Optimization of nonpneumatic tire with hexagonal lattice spokes for reducing rolling resistance. SAE Tech Pap. 2015:2015-01-1515.
[12] Shida Z, Koishi M, Kogure T, Kabe K. A rolling resistance simulation of tires using static finite element analysis. Tire Sci Technol. 1999;27(2):84-105.
[13] Kusaka K. Estimation of tire rolling resistance using statistical tire modeling method and its validation. Trans Soc Automot Eng Japan. 2019;50(5):1343-1348.
[14] Hotaka T, Sakai T. Tire rolling resistance correction technology taking viscoelastic characteristics into consideration. Trans Soc Automot Eng Japan. 2019;50(6):1581-1586. (In Japanese)
[15] Nakajima Y. Advanced tire mechanics. Singapore: Springer; 2019.
[16] Suzuki T, Sasaki K, Okano T, Washimi Y. Reduction of rolling resistance by airless tire with linked zig zag structure. JSME annual meeting; 2023 Sep 4-6; Tokyo, Japan. Japan: Japan Society of Mechanical Engineering; 2023. p. J191-12. (In Japanese)
[17] Ju J, Summers JD. Compliant hexagonal periodic lattice structures having both high shear strength and high shear strain. Mater Des. 2011;32(2):512-524.
[18] Kim K, Kim D. Contact pressure of non-pneumatic tires with hexagonal lattice spokes. SAE Tech Pap. 2011: 2011-01-0099.

[19] Yokoyama K, Ushijima K, Suzuki T, Sasaki K, Okano T, Washimi Y. Evaluation of mechanical properties of linked zig-zag structure subjected to in-plane compressive load. The Proceedings of Mechanical Engineering Congress, Japan. 2023;89(927):23-00216. (In Japanese)